Synthesis of the Polycation Thymidyl DNG, Its Fidelity in Binding Polyanionic DNA/RNA, and the Stability and Nature of the Hybrid Complexes

Robert O. Dempcy, Kenneth A. Browne, and Thomas C. Bruice*

Department of Chemistry, University of California Santa Barbara, California 93106

Received February 22, 1995

Putative drugs consisting of oligonucleotide analogs capable of combining with RNA or DNA, thereby arresting cellular processes at the translational or transcriptional level, are known as antisense and antigene agents.[1] The backbones of viable antisense/antigene agents do not incorporate phosphodiester linkages because of the susceptibility of this linkage to degradation by cellular nucleases. To be effective, such agents must bind with fidelity to target nucleic acids *via* Watson−Crick and Hoogsteen base pairing. Since antisense/antigene agents must compete with specific oligonucleotides and proteins for RNA/DNA targets, it is desirable that these agents bind with high affinity to compatible RNA/DNA sequences. The stability of double- and triple-stranded RNA and DNA would increase if the electrostatic repulsion among the polyanionic single strands could be alleviated. This is seen in the enhanced binding of the neutrally charged peptide nucleic acids (PNA) to ssDNA.[2] One might suspect, therefore, that a strand complementary to DNA and connected together by positively charged linkages would act as a particularly effective antisense/antigene agent since the repulsive electrostatic effects in dsDNA would be replaced by attractive electrostatic interactions. On the other hand, the electrostatic bonding between polycationic and polyanionic structures might be quite nonspecific and independent of complementary base pairing. We report herein the synthesis of the pentameric thymidyl deoxyribonucleic guanidine (DNG) **1** in which the phosphodiester linkages of DNA [$-O(PO_2^-)O-$] are replaced by guanidinium linkages [$-NHC(=NH_2^+)NH-$]. Preliminary results indicate that this DNG model compound exhibits complementary base pair recognition toward both RNA and DNA, and the double- and triple-helical structures composed of DNG with RNA or DNA demonstrate unprecedented stability. One should note that DNG is expected to be stable *in vivo* due to the absence of phosphodiester linkages.

The synthesis of **1** (Scheme 1) was accomplished *via* a cyclic process starting with a condensation reaction between 3′-amino-5′-*O*-trityl-3′-deoxythymidine[3] (**2**) and 3′-azido-5′-isothiocyano-3′,5′-deoxythymidine (**3**), affording the 5′ → 3′ thiourea-linked dimer **4**. The synthesis of **3** was carried out by the reaction of 5′-amino-3′-azido-3′,5′-deoxythymidine with carbon disulfide in the presence of DCC. Chain extension from the dimer followed a cyclic two-step process involving reduction of the 3′-azido moiety with hydrogen sulfide. The resulting amine was then condensed with another equivalent of **3**. The thiourea-linked thymidyl pentamer was converted to **1** by oxidation of the thiourea linkages to aminoiminosulfonic acid linkages followed by amination with ammonium hydroxide and purification.[4] The polycationic nature of **1** is shown by its electrophoretic mobility toward the anode, in contrast to DNA migration, which is toward the cathode.

Scheme 1

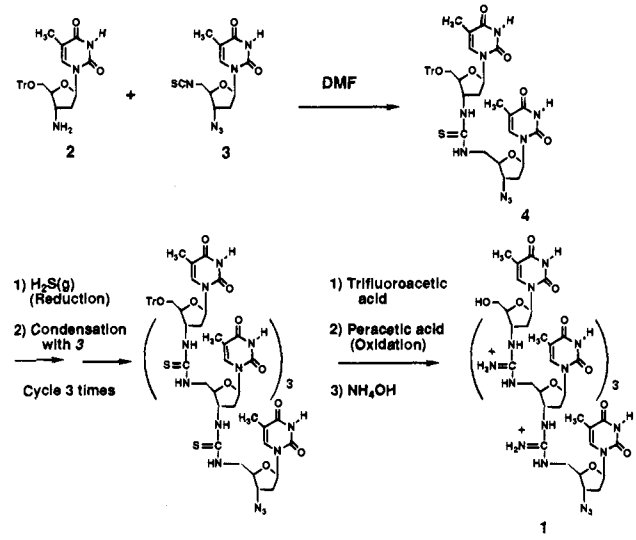

The energy-minimized structure for the DNA·DNG complex $d(pA)_{10}$·$d(gT)_{10}$ (where "g" indicates a guanidyl linkage instead of a phosphate "p") primarily retains a B-DNA conformation with the minor groove contracted by the electrostatic attraction between the $-O(PO_2^-)O-$ and $-NHC(=NH_2^+)NH-$ units.[5] The energy-minimized structure for the RNA·DNG complex $r(Ap)_9A$·$d(Tg)_9T$−azido (Figure 1) adopts an A-type structure with sugars of both strands in the C3′-endo conformation. As was expected and also seen with the DNA·DNG complex,[5] the minor groove of the RNA·DNG complex is contracted (the minor groove width decreases by ca. 1.4 Å) due to electrostatic interactions between the backbone moieties. Computational studies establish that triple-helical structures are also possible between two DNG strands and one DNA or RNA strand.

In the thermal denaturation analysis of **1** bound to poly(dA) or poly(rA), the plot of absorbance at 260 nm (A_{260}) vs temperature exhibits two distinct inflections (Figure 2). On this basis, we reasonably assign the plots in Figure 2 to represent denaturation curves of triple- and double-helical structures of **1** with ssDNA [$\mathbf{1}_2$·poly(dA) and **1**·poly(dA)] and ssRNA [$\mathbf{1}_2$·poly(rA) and **1**·poly(rA)]. Further support for this assignment is provided by the dependence of the thermal denaturation temperatures (designated by T_m) on ionic strengths. Denaturation of the triple helix $\mathbf{1}_2$·poly(dA) occurs at 68, 41, and 36 °C when μ = 0.22, 0.62 and 1.2, respectively, followed by denaturation of the **1**·poly(dA) duplex at 79, 70, and 71 °C. At μ = 0.12, only one transition was seen centered at 85 °C; the thermal stability is apparently so great that the double-helical structure does not denature at near boiling temperatures. The thermal denaturation curves for $\mathbf{1}_2$·poly(rA) and **1**·poly(rA) also show two inflections [T_{m1} = 63, 44, 50, and 53 °C for the $\mathbf{1}_2$·poly(rA) → **1**·poly(rA) + **1** transition and T_{m2} = ∼100 (estimated), 91, 90, and 82 °C for the **1**·poly(rA) → poly(rA) + **1** transition at μ = 0.22, 0.62, 0.82, and 1.2, respectively]. At μ = 0.12, no transitions were seen as high as 93 °C; the thermal stability is so great that neither double- nor triple-stranded structures denature at near-boiling temperatures. The T_m values of **1**·poly(rA) are higher than seen in the case of the corresponding DNA·RNA complexes. For solutions which contained **1** and either $p(dG)_{12-18}$, poly(rG), poly(dC), poly-

(1) (a) Uhlmann, E.; Peyman, A. *Chem. Rev.* **1990**, *90*, 543. (b) Crooke, S. T. *Annu. Rev. Pharmacol. Toxicol.* **1992**, *32*, 329. (c) Crooke, S. T. *FASEB J.* **1993**, *7*, 533. (d) Cook, P. D. *Antisense Research and Applications*; Crooke, S. T., Lebleu, B., Eds.; CRC: Boca Raton, 1993; pp 149−187. (e) Sanghvi, Y. S.; Cook, P. D. In *Nucleosides and Nucleotides as Antitumor and Antiviral Agents*; Chu, C. K., Baker, D. C., Eds.; Plenum: New York, 1993; pp 311−324.

(2) (a) Nielsen, P. E.; Egholm, M.; Berg, R. H.; Buchardt, O. *Science* **1991**, *254*, 1497. (b) Almarsson, Ö.; Bruice, T. C.; Kerr, J.; Zuckermann, R. N. *Proc. Natl. Acad. Sci. U.S.A.* **1993**, *90*, 7518.

(3) Glinski, R. P.; Khan, M. S.; Kalamas, R. L.; Sporn, M. B. *J. Org. Chem.* **1973**, *38*, 4299. The 3′-azido analog in this reference was reduced with Pd/C, H_2(g) in ethanol.

(4) Purification of **1** was carried out by preparative HPLC using an Alltech WCX cation exchange column employing 0.80 M ammonium acetate buffer, pH 5.0, as the mobile phase. Evidence for the successful conversion of the thiourea linkages to the corresponding guanidinium linkages was established by ^{13}C NMR (the guanidinium carbons are observed around 155 ppm) and mass spectral analysis [*m/e* 1328.60 $(M + H)^+$, calcd 1328.56].

(5) Dempcy, R. O.; Almarsson, Ö.; Bruice, T. C. *Proc. Natl. Acad. Sci. U.S.A.* **1994**, *91*, 7864.

0002-7863/95/1517-6140$09.00/0

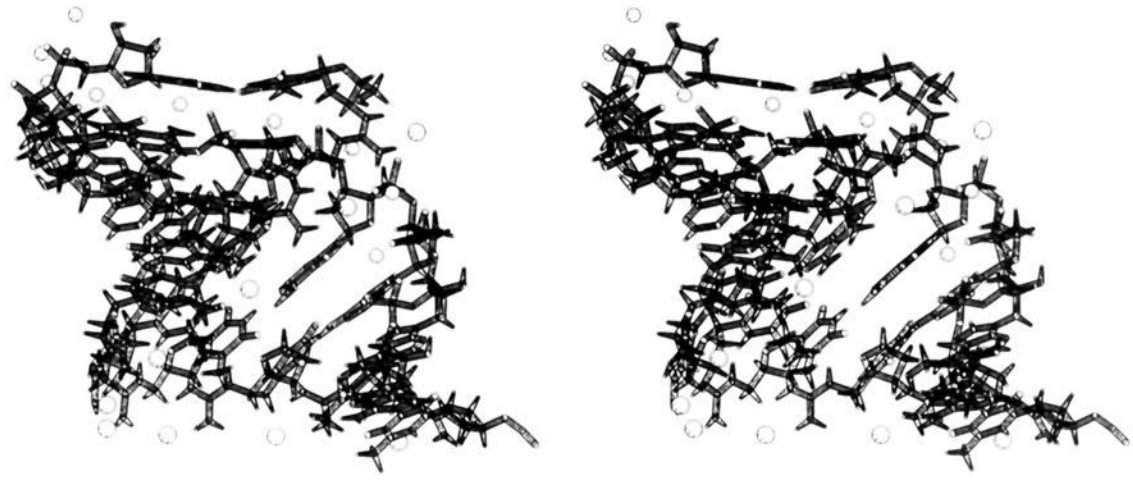

Figure 1. Stereoview of the duplex hybrid of r(Ap)$_9$A·d(Tg)$_9$T−azido. The model was computer generated from an initial structure of A-type d(Ap)$_9$A·d(Tp)$_9$T, converting the H2′ groups of the purine strand into hydroxyl groups, and replacing the phosphate linkages of the pyrimidine strand with guanidyl linkages. Explicit Cl^- and Na^+ counterions were included. The adopted-basis Newton Raphson algorithm was used to energy minimize using CHARMm version 21.3 until the root mean square derivative reached <0.5 kcal mol^{-1} Å^{-1}.

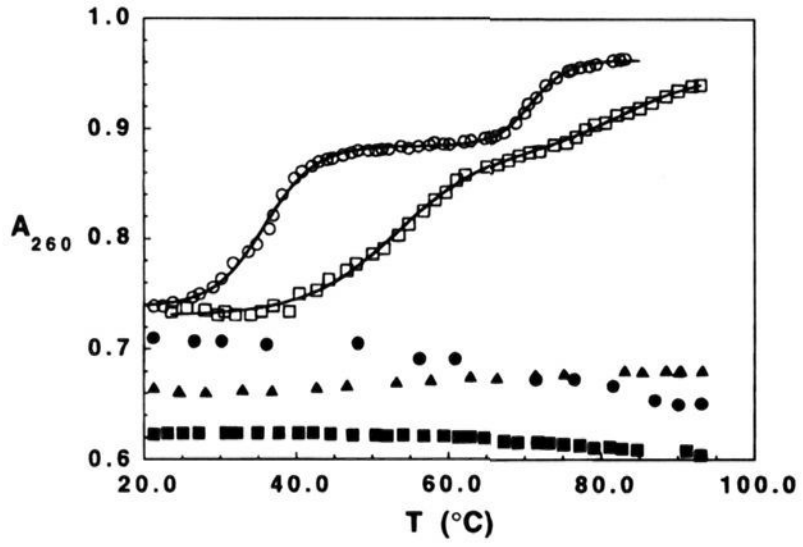

Figure 2. Plots of A_{260} vs T (°C) for d(Tg)$_4$T−azido (**1**) annealed to poly(dA) (○), poly(rA) (□), p(dG)$_{12-18}$ (●), poly(rC) (■), or poly(rU) (▲) at pH 7.0 (0.01 M $KHPO_4$ buffer) and an ionic strength of 1.2 (KCl). The concentration of each of the oligonucleotides was 4.17 × 10^{-5} M in bases. The change in absorbance (260 nm) with increasing temperature was monitored using a Perkin-Elmer 553 spectrophotometer. The temperature was controlled by circulating water from a Haake RM3T thermostated water bath through water-jacketed cuvette holders in the spectrophotometer. The temperature of the solutions in the cuvettes was monitored with a NIST digital thermometer (accurate to ±0.2 °C). Data points were collected in ca. 1 °C increments at ca. 5 min intervals (larger temperature increments for nonspecific polynucleic acids). The data points which comprise the curves for complexes of d(Tg)$_4$T−azido with poly(dA) and poly(rA) were then computer fitted to an equation for two inflection points (T_{m1} and T_{m2}).

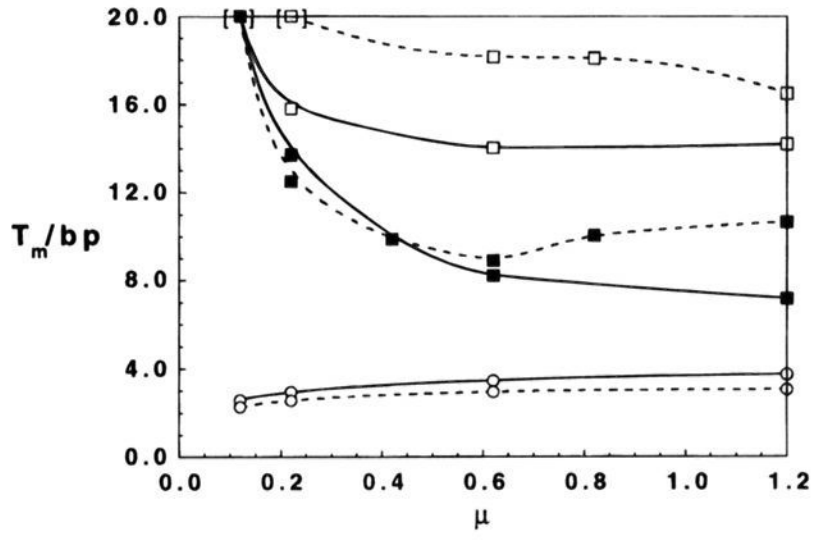

Figure 3. A plot of T_m/base pair vs ionic strength (μ varied with different [KCl]) at pH 7.0 (0.01 M $KHPO_4$ buffer) for denaturation of d(Tg)$_4$T−azido (■ and □ for the first and second transitions, respectively) and d(Tp)$_{15}$T (○) complexed to poly(dA) (—) and poly(rA) (- - -). The data point at the lowest ionic strength for the nucleic complexes with DNG was taken as 100 °C because no hyperchromic transition was apparent up to 93 °C.

(rC), or poly(rU), no hyperchromic shift at 260 nm was observed between ca. 5 and 93 °C with varying ionic strength at pH 7.0 (Figure 2). This argues against noncomplementary binding of the thymine bases of **1** to DNA or RNA. From these preliminary results, DNG appears to interact with DNA and RNA with specificity in forming hybrid duplex and triplex structures.

Not only does **1** have a significantly greater affinity for poly(dA) and poly(rA) than does thymidyl DNA, but the effect of ionic strength on stability is more pronounced. As one might expect, we find that the ionic strength has an opposite effect on the T_m values of DNG hybrids with DNA or RNA as compared to DNA complexes with DNA or RNA since electrostatic interactions are attenuated by increasing salt concentration. In Figure 3, plots of T_m/(number of base pairs) vs ionic strength are shown. Analysis of Figure 3 indicates that the triple-helical DNG$_2$·DNA and DNG$_2$·RNA complexes have similar stability while the DNG complex with RNA is more stable than the corresponding DNG·DNA complex.

In summary, we show in these preliminary investigations that the attractive forces between negatively charged DNA or RNA and positively charged DNG contribute significantly to the stability of heteroduplex and heterotriplex structures formed between these species. The differing influence of increase in ionic strength on the stability of duplex and triplex structures composed of DNA and/or RNA, as compared to such structures composed of DNG in combination with DNA or RNA, supports the importance of charge attraction and repulsion in determining stability of triplex and duplex structures. An increase in ionic strength shields electrostatic interactions, hence, decreasing the force between positive and negative charges. The repulsion between negative charges found on opposite strands of DNA and RNA duplex and triplex structures diminishes with increasing μ such that stability (T_m) increases with increasing μ. In the case of structures of DNG with DNA or RNA, the attractive forces between positive DNG and negative nucleic acid increase with decreasing μ. Thus, DNG duplex and triplex structures with DNA or RNA are much more stable at physiological ionic strength than the corresponding structures with DNA and RNA as the sole components. Regardless of the uniquely tight binding of DNG to DNA or RNA, there is a yet to be completely defined fidelity of base pair recognition. The thymine of the DNG pentamer **1** recognizes adenine but not guanine or cytosine. These features encourage us toward further characterization of DNG and its RNA analog RNG as putative antisense/antigene agents.

Acknowledgment. This work was supported by the National Science Foundation and the Office of Naval Research.

JA950615+